Available online at www.sciencedirect.com
ScienceDirect
Tetrahedron 63 (2007) 7916–7925
Tetrahedron

Synthesis of three-dimensionally arranged porphyrin arrays via intramolecular *meso–meso* coupling

Goro Mori, Naoki Aratani and Atsuhiro Osuka*

Department of Chemistry, Graduate School of Science, Kyoto University, Sakyo-ku, Kyoto 606-8502, Japan

Received 4 April 2007; revised 17 May 2007; accepted 18 May 2007
Available online 24 May 2007

Abstract—The synthesis and photophysical properties of three-dimensionally arranged porphyrin arrays with through-space electronic communication are reported. 1,3,5-Trioxamethylphenylene bridged Zn(II) porphyrin trimer **3** was coupled by Ag(I)-promoted oxidative coupling reaction to give porphyrin cage **5** comprising three *meso–meso* linked diporphyrins, which was then transformed by oxidation with DDQ and $Sc(OTf)_3$ into porphyrin cage **7** comprising three fused diporphyrins. Intramolecular *meso–meso* coupling reaction was applied to porphyrin pentamer **11** to provide porphyrin array **12** consisting of a porphyrin core flanked by two *meso–meso* linked diporphyrins. Further oxidation of **12** with DDQ and $Sc(OTf)_3$ afforded triply stacked porphyrin array **13** that is comprised of a porphyrin core flanked by two porphyrin tapes. UV–vis–NIR absorption and fluorescence spectra of **5**, **7**, **12**, and **13** showed their distorted conformations and electronic interaction within the stacked porphyrin arrays.

1. Introduction

In recent years, a variety of covalently-linked porphyrin arrays have been explored in light of their uses as biomimetic models of photosynthetic systems, conductive organic materials, near-infrared dyes, nonlinear optical (NLO) materials, molecular wires, and functional molecular devices.[1] Among these, we reported the Ag(I)-promoted coupling reaction of a 5,15-diaryl Zn(II) porphyrin as a versatile method that enables the synthesis of very long yet discrete *meso–meso* linked porphyrin arrays.[2] They are attractive as a molecular wire owing to the linear shape, the small HOMO–LUMO gap of a constitutional porphyrin, and the large electronic interaction between the neighboring porphyrin subunits arising from the direct linkage.[2] This method is also applicable for intramolecular coupling.[3–5] Intramolecular cyclization reaction of *m*-phenylene bridged porphyrin arrays has been shown very effective to construct medium and large porphyrin rings, in which efficient excitation energy hopping is realized along the wheel.[4,5]

We also developed the fusion reaction of *meso–meso* linked diporphyrins to *meso–meso*, β–β, β–β linked diporphyrins (porphyrin tapes) by oxidation with DDQ and $Sc(OTf)_3$.[6] Porphyrin tapes have been demonstrated to have great promise for a variety of photonic applications, exhibiting the lowest absorption bands that reach the infrared region.[7] Specifically, this feature is of great advantage of NLO properties, and fused porphyrin dimers actually have the highest class of two-photon absorption (TPA) cross-section value (δ) of ~15,000 GM.[7] Porphyrin tapes are also the current focus of intensive researches, because they have been used for the construction of functional conjugates with fullerenes due to specific supramolecular interactions.[8,9] However, incorporation of the porphyrin tape unit into more sophisticated molecular systems has been rather limited. An interesting example is a cyclic porphyrin tape developed by Tashiro et al.[8] They showed a positive heterotropic host–guest system, where the guests with complementary electronic effects on the binding properties of porphyrin tapes are allowed to communicate with one another through the π-electronic conjugation. Another example is the surface modification patterned by a porphyrin tape that can arrange C_{60} in the solid state.[9]

Here we report the Ag(I)-promoted coupling reaction of 1,3,5-trioxamethylphenylene-bridged Zn(II) triporphyrin **3** as a prototype of spacer-directed synthesis of porphyrin cage. This type of coupling reaction makes it feasible that the overall molecular shape and the magnitude of the electronic interaction of porphyrin arrays can be dictated by the design of an appropriate spacer, thus enhancing the synthetic potential of this coupling reaction.[10] In next step, this strategy has been extended to porphyrin pentamer **11**, in which the central Zn(II) porphyrin core bears four *meso*-free Zn(II) porphyrins.

Keywords: π-Conjugated system; Porphyrinoid; Cage molecule; Oligomers.
* Corresponding author. Tel.: +81 (0)75 753 4008; fax: +81 (0)75 753 3970; e-mail: osuka@kuchem.kyoto-u.ac.jp

0040–4020/$ - see front matter © 2007 Elsevier Ltd. All rights reserved.
doi:10.1016/j.tet.2007.05.075

2. Results and discussion

2.1. Synthesis and photophysical properties of concurrently stacked porphyrin hexamers

1,3,5-Tris[4′-(tosyloxy)-2′-oxa-1′-butyl]benzene (**2**) was prepared according to the published procedure.[11] The pendant porphyrin **1** was prepared from the corresponding methoxy compound with BBr_3 in 89% yield. Compounds **1** and **2** were coupled under the standard ether synthetic conditions (NaOH and DMF) and subsequent separation over GPC followed by zinc metallation afforded the trimer **3** in 71% yield (Scheme 1). The structure of **3** was confirmed by ^{1}H NMR spectroscopy and MALDI-TOF-MS.

Then, we attempted the Ag(I)-promoted coupling reaction of the porphyrin **3**. Under the standard conditions (**3** 0.38 mM, $AgPF_6$ 0.63 mM, $CHCl_3$, 50 min, room temperature),[2] hexameric porphyrin **4** was obtained in 27% yield along with recovery of **3** (67%) (Scheme 2). Next, intramolecular coupling reaction of **4** was carried out with 2.0 equiv of $AgPF_6$ under high dilution (1.8×10^{-6} M) for 36 h at room temperature. Progress of the reaction was monitored by analytical GPC–HPLC, which revealed the formation of a discrete product that eluted as a shoulder at 21.7 min, later than **4** (20.8 min) (Fig. 1). This product was isolated by repeated separations using preparative GPC–HPLC in 38% yield, and was assigned to be hexameric porphyrin cage **5**, on the basis of the following facts. (1) The product exhibits the parent ion peak at m/z=5533 in MALDI-TOF mass spectrum, indicating its hexameric porphyrin constitution. (2) Despite almost the same molecular weight, a distinct difference in the retention time on the GPC–HPLC from **4** indicates a substantial difference in the hydrodynamic volume, which could arise from an overall drastic change in molecular shape. Finally, (3) the ^{1}H NMR spectrum of **5** is quite simple, featuring only single set of a porphyrin subunit, indicating its high molecular symmetry. Importantly, the outer and inner porphyrinic β-protons are all distinguished owing to restricted rotation. All the signals were assigned by experimentally observed coupling connectivity. The spectrum shows good accordance with the C_3-symmetric structure, in which the

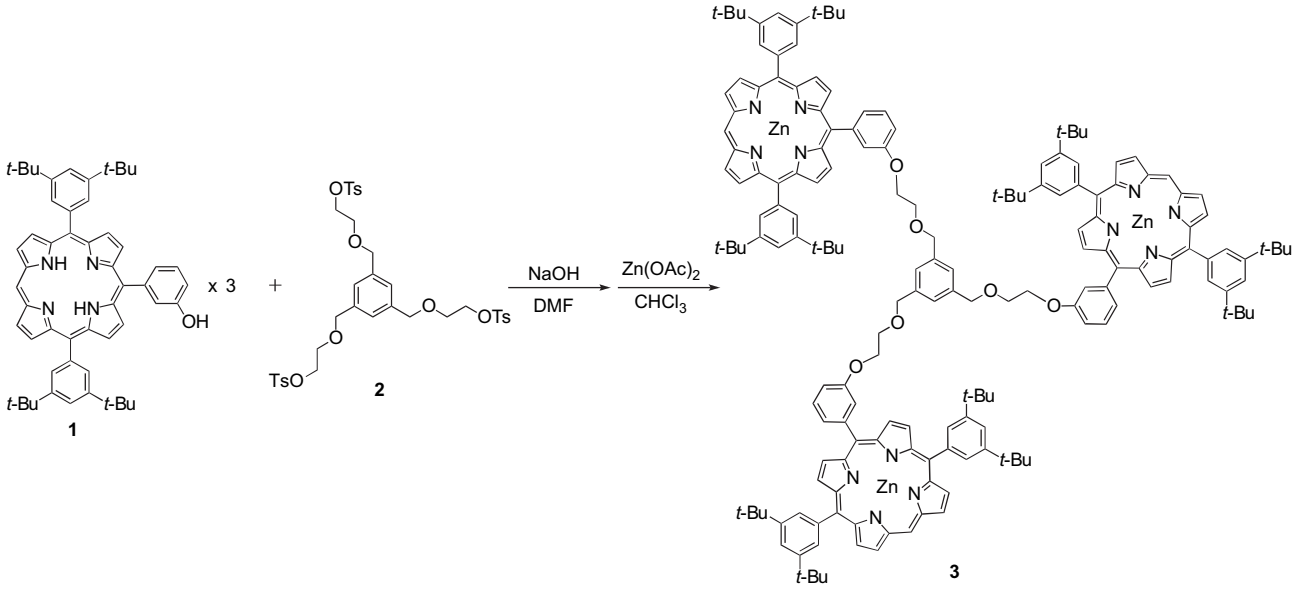

Scheme 1. Synthesis of bridged porphyrin trimer **3**.

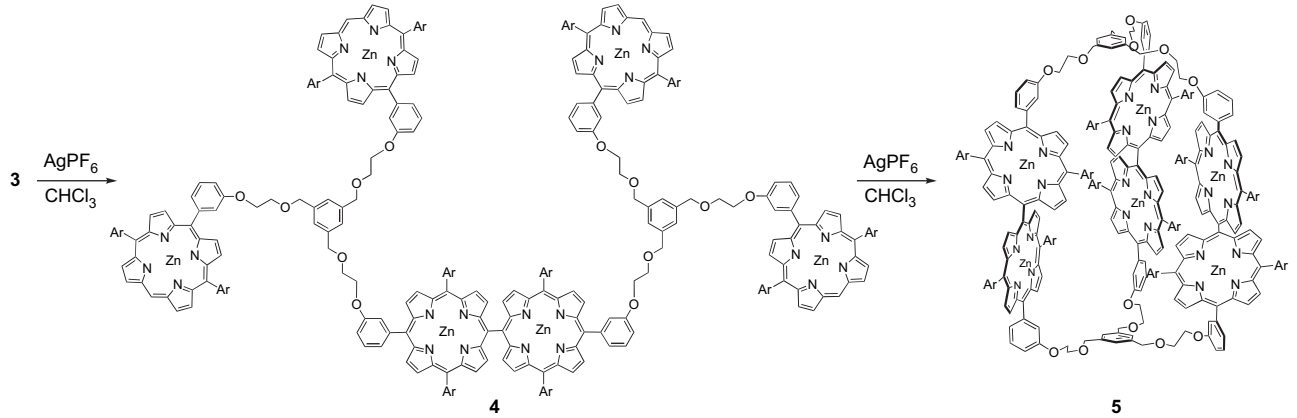

Scheme 2. Synthesis of bridged porphyrin hexamers, Ar=3,5-di-*tert*-butylphenyl.

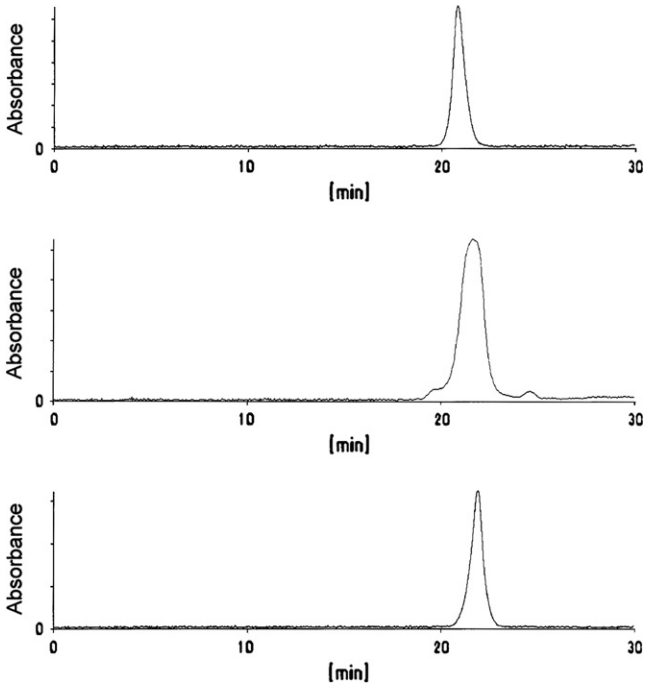

Figure 1. GPC chromatograms of the coupling reaction of porphyrin hexamer **4** (JAIGEL 2.5H-AF, 3H-AF, and 4H-AF, flow rate=1.2 mL min^{-1}, 35 °C eluted with THF).

characteristic signals are observed at −0.5 and +0.5 ppm, which are assigned to the *tert*-butyl protons. Such a large high field shift suggests considerable proximity of the *tert*-butyl protons to the neighboring porphyrin ring.

The optimized molecular structure by the AM1 calculation indicates a folded C_3-conformation with close contact between six porphyrins as shown in Figure 2.

Figure 3 shows the UV–vis absorption and fluorescence spectra of **5** taken in $CHCl_3$. For comparison, the spectra of *meso–meso* linked Zn(II) diporphyrin **6** are shown together. Similar to the reference diporphyrin **6**, the hexamer **5** shows the split Soret band (λ_{max}=423 and 453 nm) and the Q band at 555 nm. Interestingly, the low-energy Soret band of **5** is smaller and blue-shifted as compared to that of **6**, whereas the high-energy Soret band and the Q-bands of **5** are similar to those of **6**. The fluorescence spectrum of **5** taken for excitation at 420 nm displays a band at 653 nm with a shoulder peak around 610 nm, which is similar to that of **6** with respect to observed position but different with respect to spectral shape. In addition, the relative fluorescence quantum yield of **5** is 0.025, being less than half of **6** (Φ_F=0.052).[12]

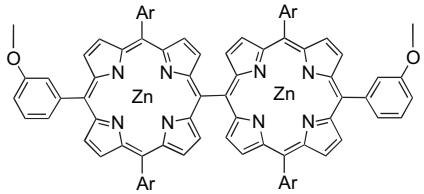

6 Ar = 3,5- di-*tert*-butylphenyl

The characteristic split Soret band of *meso–meso* linked Zn(II) diporphyrins can be accounted in terms of exciton

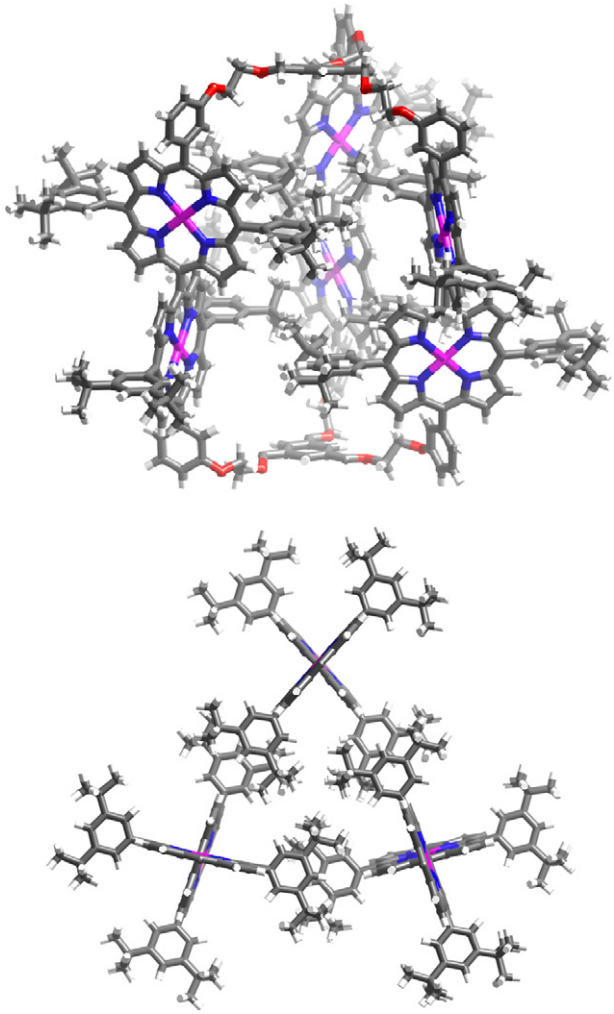

Figure 2. Optimized structure of porphyrin hexamer **5**; top: side view, bottom: top view. Bridging units in the top view are omitted for clarity.

coupling as shown in Scheme 3.[13] The Soret band of a Zn(II) porphyrin has two perpendicular components B_x and B_Y. In a simple monomer (Scheme 3a) they are degenerate, but in a *meso–meso* linked diporphyrin (Scheme 3b), they couple differently. In the case of dimer, B_x transition dipole moments along the *meso–meso* linkage are excitonically coupled to generate an allowed lower energy transition (B_x+$B_{x'}$), while the mutual Coulombic interactions of B_Y and B_Z transition dipole moments do not interact due to their orthogonal conformation. Consequently, Soret band of *meso–meso* linked linear porphyrin arrays are split into a red-shifted band and an unperturbed band (Scheme 3). The similar interactions can be considered for Q-bands, but the spectral changes of Q-bands are quite small due to the much smaller oscillator strength of Q-bands than those of B-band. The absorption and fluorescence spectra of **5** cannot be explained by decreased dihedral angle of the *meso–meso* linkage, since such diporphyrins show different spectral characteristics, gradual changes into four Soret bands, and fluorescence red shifts upon the extent of decrease in the dihedral angle (Scheme 3d).[14] We, therefore, consider the bending of *meso–meso* linked diporphyrins along their long molecular axis (Scheme 3c), which may be caused by clipping three *meso–meso* linked diporphyrins at the two

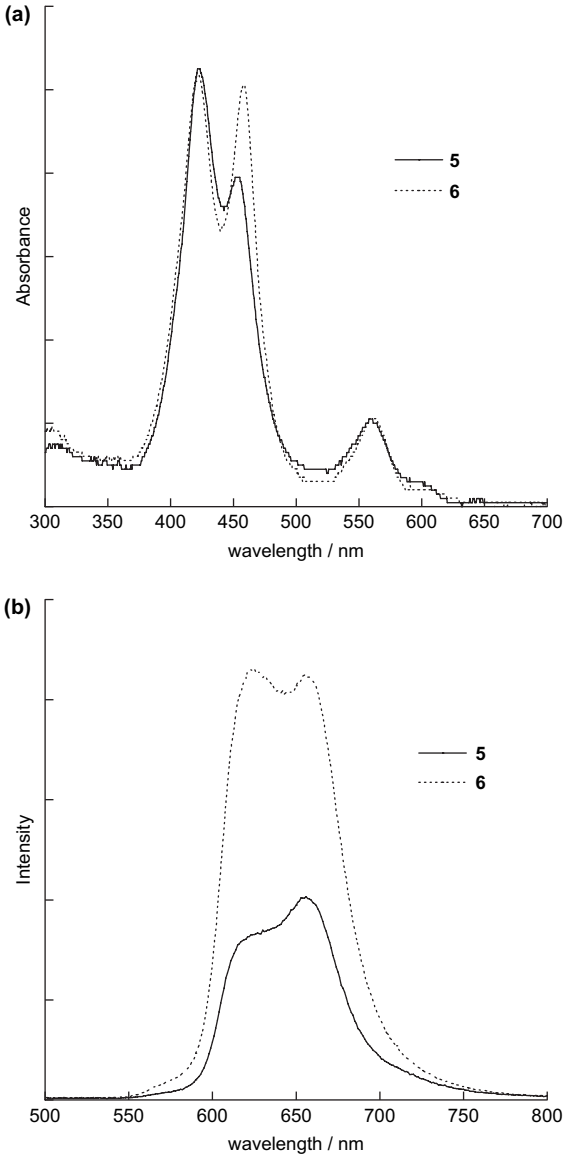

Figure 3. (a) UV–vis absorption spectra of **5** and **6** taken in $CHCl_3$. The absorbances at ca. 420 nm were normalized. (b) Fluorescence spectra of **5** and **6** taken upon excitation at 420 nm with the absorbance adjusted at 0.10.

sites in solution. Such a kink structure has been often proposed for energy sink that disrupts excitation energy hopping along the *meso–meso* linked Zn(II) porphyrin arrays[15] and is likely consistent with the observed decreased fluorescence quantum yield of **5** as compared with that of **6**.

In next step, the porphyrin hexamer **5** was oxidized with $Sc(OTf)_3$–DDQ to perform fusion reaction of *meso–meso* linked diporphyrins to the corresponding *meso–meso*, β–β, β–β triply fused diporphyrins. In toluene, **5** was treated with 15 equiv of DDQ and $Sc(OTf)_3$ at 60 °C for 12 h followed by separation over a short alumina column to provide **7** as black solids in 48% yield (Scheme 4). The structure was characterized by ^{1}H NMR, MALDI-TOF-MS, and UV–vis–NIR absorption spectra. The optimized molecular structure of **7** by the AM1 calculation also indicates a folded C_3-conformation with close contact between six porphyrins as shown in Figure 4.

The absorption spectrum of **7** is slightly blue-shifted compared to that of fused diporphyrin **8** probably because of its parallel arrangement, thus indicating weak but distinct through-space electronic interaction between fused diporphyrins (Fig. 5). This result is interesting from a viewpoint that the fusion reaction is possible even for this sort of sterically constrained system.

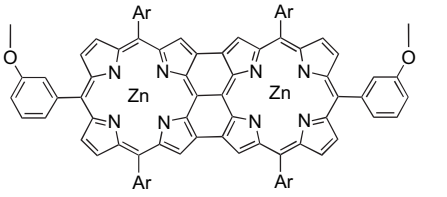

8 Ar = 3,5-di-*tert*-butylphenyl

2.2. Synthesis and photophysical properties of triply stacked porphyrin pentamers

Next we tried to make more effectively through-space interactive porphyrin oligomers, for which we designed a new precursor that has alkyl chains of precise length for intramolecular coupling.

Synthesis of pentamer **11** is shown in Scheme 5. Alkylation of 3-hydroxybenzaldehyde was performed by a Williamson type reaction to give 3-(3′-bromopropyloxy)benzaldehyde (**9**). The porphyrin **10** was prepared from **9** and pyrrole in 10% yield under the standard Lindsey conditions. Pentaporphyrin **11** was obtained as follows. A mixture of **1** (257 mg, 0.330 mmol), **10** (47.9 mg, 0.0412 mmol), and K_2CO_3 (336 mg, 2.44 mmol) in dry acetone (50 mL) was refluxed for 4 days. After removal of the solvent, the residue was purified with silica gel column chromatography. Final separation over recycling preparative GPC–HPLC gave free-base pentaporphyrin. After metallation with $Zn(OAc)_2$, zinc porphyrin pentamer **11** (87 mg, 54%) was obtained.

A *meso–meso* coupled porphyrin oligomer **12** was prepared through the one-step reaction by the Ag(I)-promoted oxidative coupling in high dilution conditions to form intramolecular coupling compound (Scheme 6). The reaction of **11** (20 mg, 4.7 μmol) with $AgPF_6$ (0.065 mmol) at room temperature in $CHCl_3$ (800 mL) for 15 h followed by preparative GPC–HPLC gave **12** (36%) and a small amount of intermolecular coupling products along with the recovery of **11**. The structural characterization of compound **12** was performed by ^{1}H NMR, MALDI-TOF-MS, GPC–HPLC, and UV–vis absorption spectrum. The symmetric structure has been indicated by its simple ^{1}H NMR spectrum at 60 °C, although that at room temperature exhibited complicated peaks probably due to rotational restriction of phenyl rings. Nine β-protons are differentiated in these porphyrin rings and their assignments have been accomplished by comprehensive ROESY measurements. High field shifted chemical shift for β-protons (6.39 ppm) can be accounted for in terms of shielding effect of the central porphyrin ring.

Next, porphyrin pentamer **12** was oxidized with $Sc(OTf)_3$–DDQ to perform fusion reaction of *meso–meso* linked diporphyrins into the corresponding *meso–meso*, β–β, β–β triply fused diporphyrins. In toluene, **12** was treated with

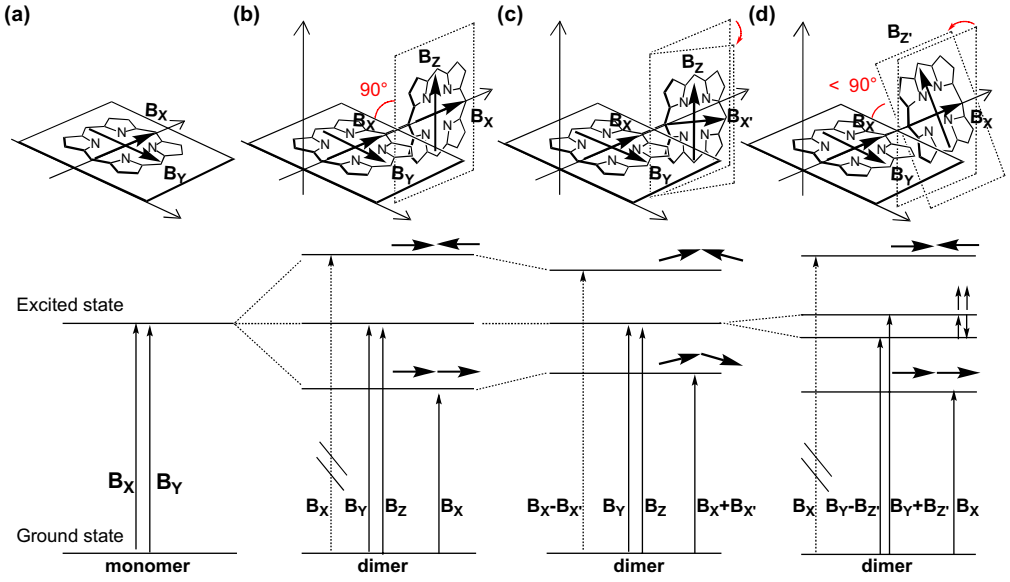

Scheme 3. Schematic energy diagrams of Zn(II) porphyrin monomer and various *meso–meso* linked Zn(II) porphyrin dimers.

10 equiv of DDQ and $Sc(OTf)_3$ at 60 °C for 36 h followed by separation over a short alumina column and GPC–HPLC to provide **13** as black solids in 10% yield (Scheme 6). The structure was characterized by ^1H NMR, MALDI-TOF-MS, GPC–HPLC, and UV–vis absorption spectrum. The optimized molecular structure of **13** by the AM1 calculation is shown in Figure 6.

UV–vis absorption and fluorescence spectra of **12** were shown in Figure 7. The absorption spectrum of **12** shows a split Soret band caused by strong exciton coupling in the *meso–meso* linked diporphyrins. Compared to the spectrum of a mixture of **14** and **6**, the spectrum of **12** showed broad absorption bands. This feature is explained on the basis of decreasing dihedral angle of the *meso–meso* linkage, which makes Soret bands broad toward both blue and red side (Scheme 3d).[14] The steady-state fluorescence spectrum of **12** exhibited an emission with a peak at 651 nm, which is quite different from either that of *meso–meso* linked diporphyrin **6** or that of 1:2 mixture of **14** and **6**, also indicating dihedral angle decreasing.

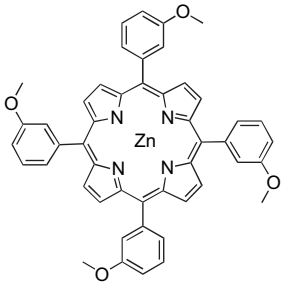

14

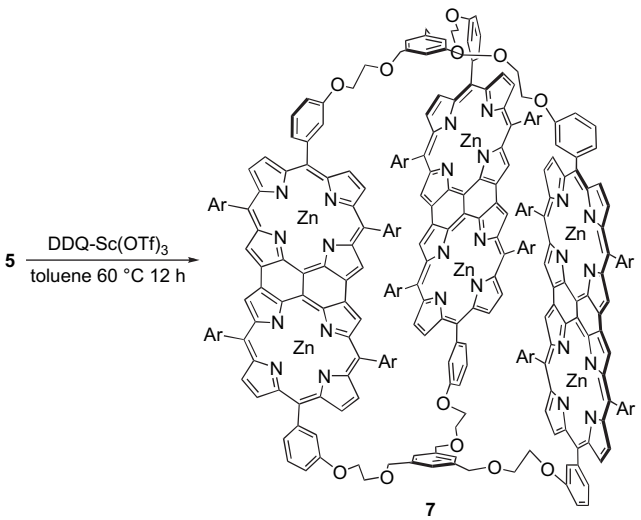

7

Scheme 4. Synthesis of **7**, Ar=3,5-di-*tert*-butylphenyl.

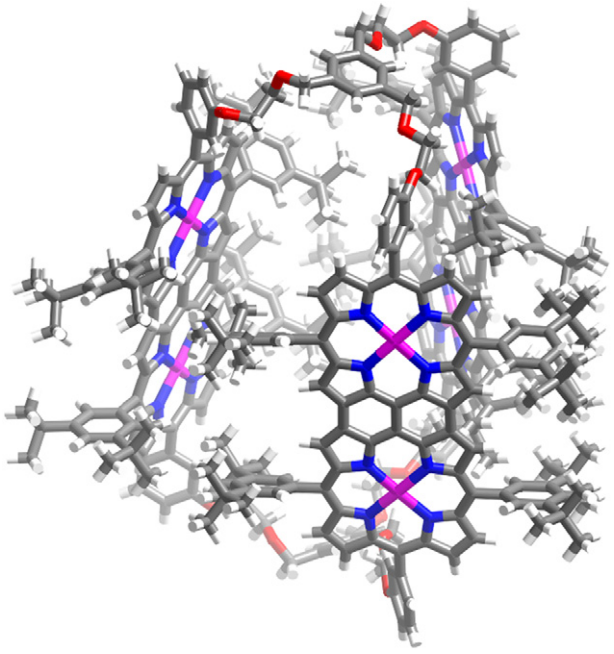

Figure 4. Optimized structure of porphyrin hexamer **7**.

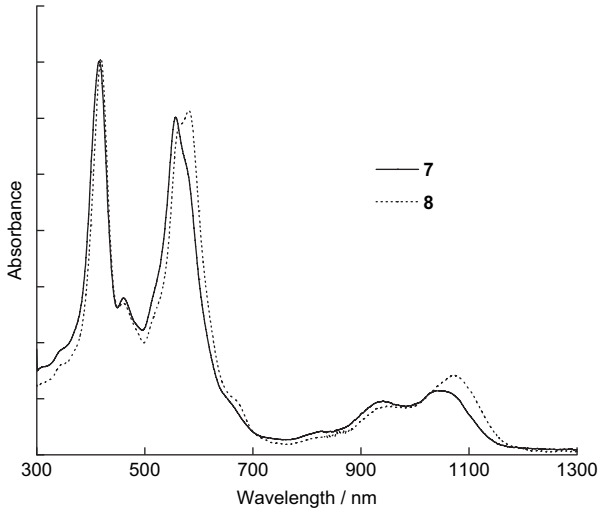

Figure 5. UV–vis–NIR absorption spectra of **7** and **8** taken in $CHCl_3$. The absorbances at ca. 420 nm were normalized.

UV–vis–NIR absorption spectrum of **13** exhibited the lowest absorption bands that reach the infrared region (Fig. 8). This is quite similar to that of a mixture of monomer **14** and dimer **8**. However, the mixture of **14** and **8** exhibited strong emissions at 600 and 648 nm from porphyrin monomer, while the fluorescence spectrum of **13** exhibited strong quenching in the range of 550–750 nm, indicating energy and/or electron transfer from the monomeric porphyrin to the *meso–meso* linked diporphyrin fragments. Here it is noteworthy that although a great number of face-to-face porphyrin dimers have been prepared so far, the synthesis of face-to-face trimers is limited to only a few examples.[16]

3. Conclusions

In summary, novel porphyrin oligomers have been prepared, where the use of 1,3,5-trioxamethylbenzene spacer led to the formation of the porphyrin cage **5** from **4** via double *meso–meso* coupling and the fusion reaction gave **7** from **5** both in acceptable yields. Inside space would be useful for guest molecules inclusion. Further work is underway to reveal the detailed photophysical properties including two-photon absorption cross-sections and to explore their host–guest chemistry. We also reported effective synthesis and photophysical properties of triply stacked porphyrin arrays by using the same strategy. In view of promises of the directly

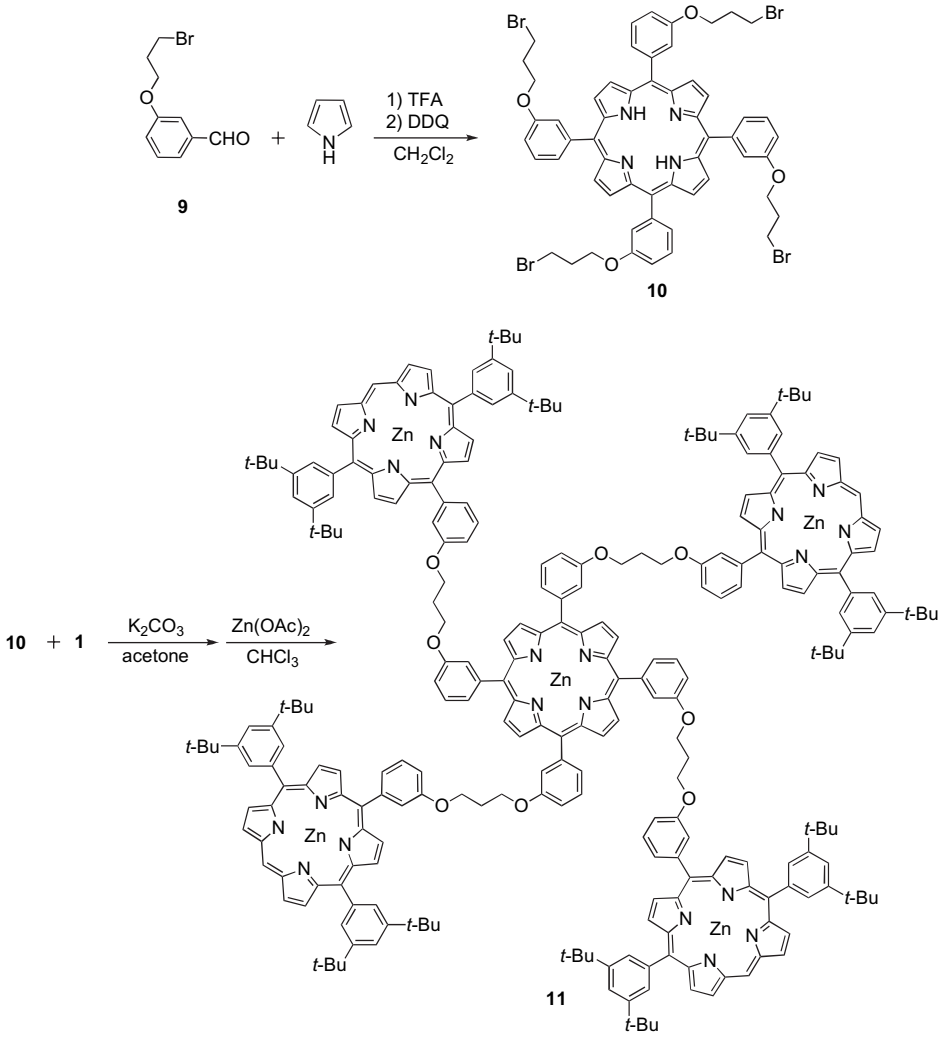

Scheme 5. Synthesis of alkyl chain bridged porphyrin pentamer **11**.

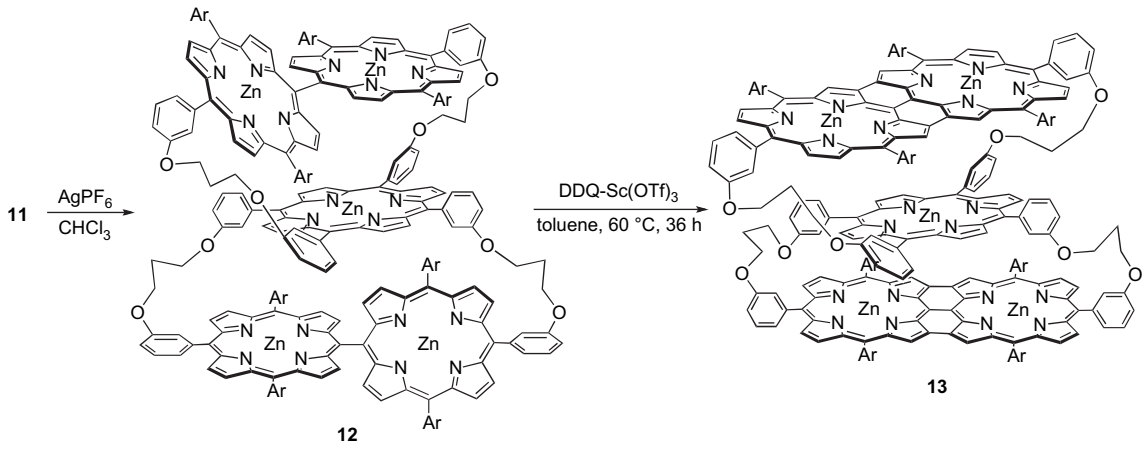

Scheme 6. Synthesis of **12** and **13**, Ar=3,5-di-*tert*-butylphenyl.

fused diporphyrin motif in various fields of material science, one of approaches to obtain higher TPA cross-section (δ) is a quasi linear donor-π-donor structure.[17] Alternatively, intramolecular face-to-face π-conjugated systems can be expected to have a large δ value due to the cofacial π-electron systems.[18] It is noteworthy that the stacked porphyrin **13** meets demands for both approaches of donor-π-donor and face-to-face structure.

4. Experimental section

4.1. General procedures

All reagents and solvents were of the commercial reagent grade and were used without further purification except where noted. Dry toluene was obtained by distillation over

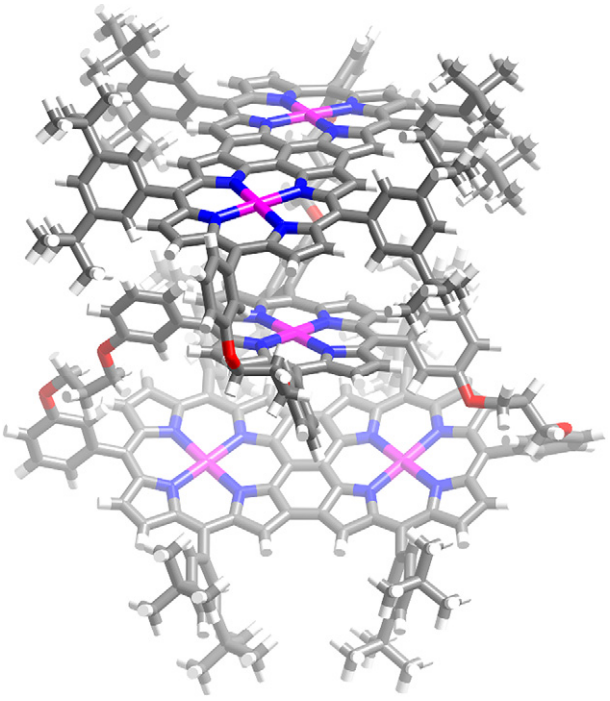

Figure 6. Optimized structure of porphyrin pentamer **13**.

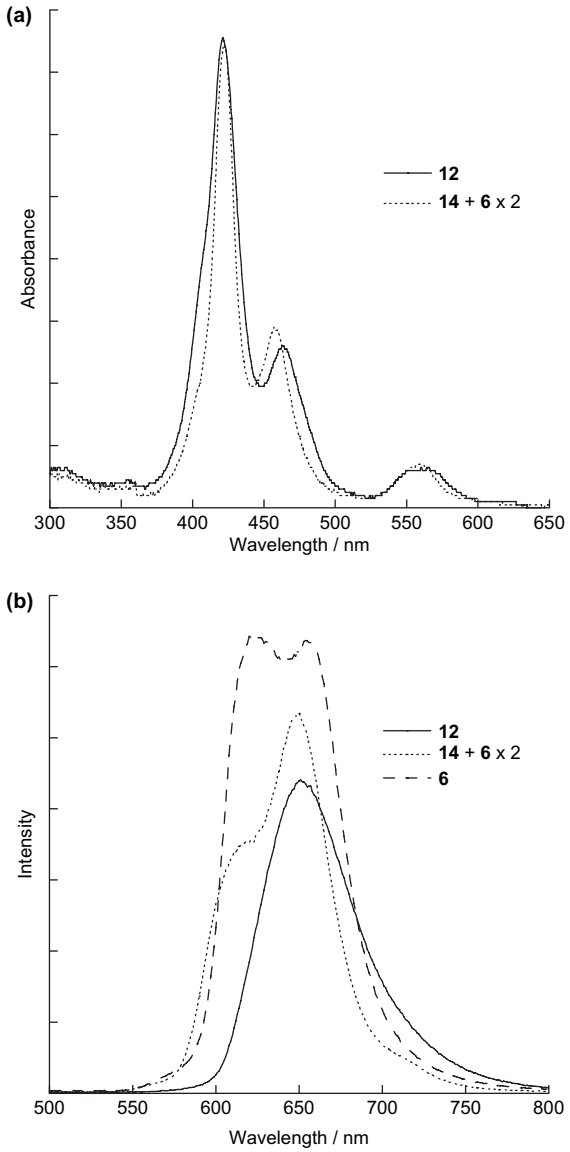

Figure 7. (a) UV–vis absorption spectra of **12** and the mixture of **14** and **6** (1:2) taken in $CHCl_3$. The absorbances at ca. 420 nm were normalized. (b) Fluorescence spectra of **12**, **6**, and the mixture of **14** and **6** (1:2) in $CHCl_3$ taken upon excitation at 420 nm with the absorbance adjusted at 0.15.

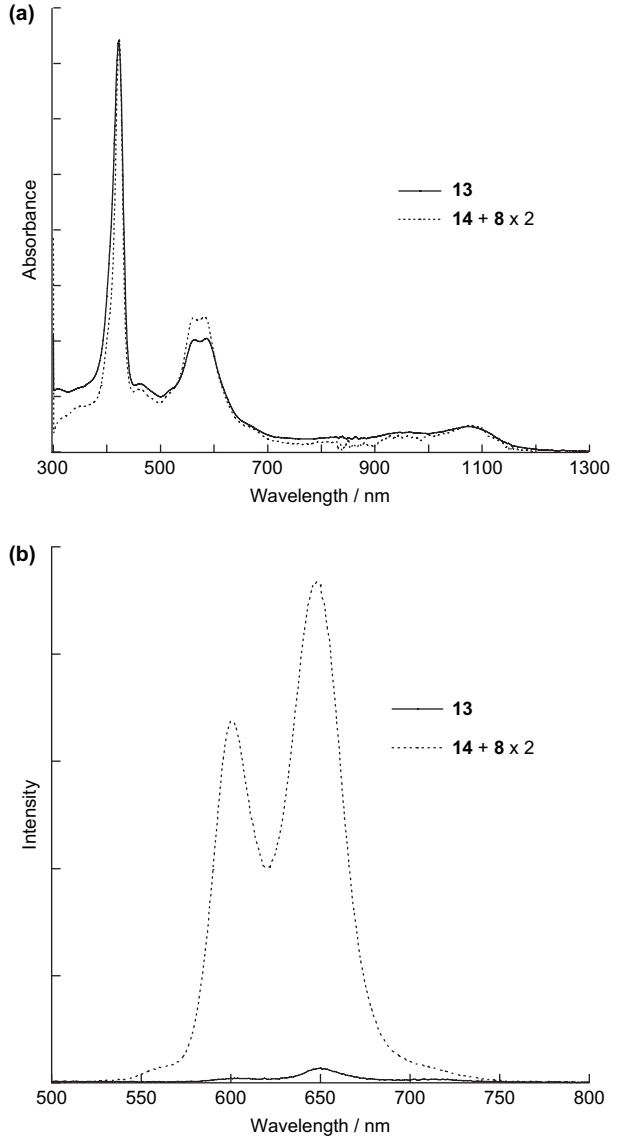

Figure 8. (a) UV–vis–NIR absorption spectra of **13** and the mixture of **14** and **8** (1:2) taken in $CHCl_3$. The absorbances at ca. 420 nm were normalized. (b) Fluorescence spectra of **13** and the mixture of **14** and **8** (1:2) in $CHCl_3$ taken upon excitation at 420 nm with the absorbance adjusted at 0.75.

CaH_2. ^1H NMR spectra were recorded on a JEOL ECA-delta-600 spectrometer, and chemical shifts were reported as the delta scale in parts per million relative to $CHCl_3$ (δ=7.26 ppm). Preparative separations were performed by silica gel gravity column chromatography (Wako gel C-300). Recycling preparative GPC–HPLC was carried out on a JAI LC-908 using preparative JAIGEL-2.5H, 3H, and 4H columns (chloroform eluant; flow rate 3.8 mL min^{-1}). The spectroscopic grade $CHCl_3$ was used as solvents for all spectroscopic studies. Steady-state UV–vis–NIR absorption spectra were recorded on a Shimadzu UV-3150 spectrometer. Mass spectra were recorded on a Shimadzu/KRATOS KOMPACT MALDI 4 spectrometer, using positive-MALDI ionization method.

4.1.1. 1,3,5-Trioxamethylbenzene-bridged zinc(II) porphyrin trimer 3. A mixture of **1** (62.3 mg, 0.08 mmol), NaOH (32 mg, 0.08 mmol), and 1,3,5-tris[4′-(tosyloxy)-2′-oxa-1′-butyl]benzene **2** (15 mg, 0.020 mmol) in dry DMF (5 mL) was stirred for 36 h at 80 °C. H_2O was added and the mixture was extracted with CH_2Cl_2. The combined organic layer was dried with Na_2SO_4 and evaporated under reduced pressure. Separation over recycling preparative GPC gave the free-base trimer. The free-base trimer was dissolved in $CHCl_3$ with $Zn(OAc)_2$ and the solution was refluxed for 3 h. After cooling, the solution was washed with water, dried with Na_2SO_4, and evaporated. After passed through a short silica gel column and evaporated the solvent, the residue was recrystallized from CH_2Cl_2/MeOH to give Zn(II) porphyrin trimer **3** (36 mg, 0.014 mmol, 71%). ^1H NMR ($CDCl_3$, 600 MHz): δ=1.50 (s, 108H, ^{t}Bu), 2.75 (t, 6H, J=4.4 Hz, CH_2), 3.13 (t, 6H, J=4.4 Hz, CH_2), 3.55 (s, 6H, CH_2), 6.21 (s, 3H, Ar-H), 6.58 (dd, 3H, J=1.8, 7.7 Hz, Ar-H), 7.30–7.34 (m, 6H, spacer-H, Ar-H), 7.61 (d, J=4.6 Hz, 3H, Ar-H), 7.70 (s, 6H, Ar-H), 8.05 (d, J=11.0 Hz, 12H, Ar-H), 8.83 (d, 6H, J=4.6 Hz, β-H), 8.96 (d, 6H, J=4.6 Hz, β-H), 9.10 (d, 6H, J=4.6 Hz, β-H), 9.32 (d, 6H, J=4.6 Hz, β-H), and 10.17 (s, 3H, *meso*-H); MALDI-TOF-MS calcd for $C_{177}H_{186}N_{12}O_6Zn_3$: 2767.25, found: 2767.25; UV–vis ($CHCl_3$): λ_{max}=418, 547, and 586 nm.

4.1.2. Zn(II) porphyrin hexamer 4. Compound **3** (200 mg, 0.072 mmol) was dissolved in $CHCl_3$ (190 mL) and the reaction vessel was covered with foil. A solution of 0.1 M $AgPF_6$ in CH_3CN (0.120 mmol) was added all at once. After stirring for 50 min at room temperature, the mixture was diluted with water and extracted with $CHCl_3$. The organic extract was washed with water and dried over anhydrous Na_2SO_4. After evaporation of solvent, the residue was dissolved with $Zn(OAc)_2$ in $CHCl_3$ and the mixture was refluxed for 3 h. The solution was washed with water, dried with Na_2SO_4, and evaporated. After passed through a short silica gel column and evaporated the solvent, separation by recycling preparative GPC–HPLC gave **3** (139 mg, 0.050 mmol, 67%) and **4** (28.1 mg, 0.0051 mmol, 27%). ^1H NMR ($CDCl_3$, 600 MHz): δ=1.46 (s, 72H, ^{t}Bu), 1.49 (s, 144H, ^{t}Bu), 2.80 (m, 4H, CH_2), 3.01 (m, 8H, CH_2), 3.13 (m, 4H, CH_2), 3.53 (m, 8H, CH_2), 3.55 (s, 4H, CH_2), 3.74 (s, 8H, CH_2), 6.39 (s, 4H, Ar-H), 6.41 (s, 2H, Ar-H), 6.65 (d, J=8.2 Hz, 2H, Ar-H), 6.72 (d, 4H, J=8.2 Hz, Ar-H), 7.35–7.40 (m, 6H, Ar-H), 7.63 (s, 2H, spacer-H), 7.65 (s, 4H, spacer-H), 7.72–7.80 (m, 18H, Ar-H), 8.04–8.11 (m, 24H, Ar-H), 8.14–8.18 (m, 4H, β-H), 8.67–8.72 (m, 4H, β-H), 8.87–8.96 (m, 24H, β-H), 9.11 (d, 8H, J=4.6 Hz, β-H), 9.34 (d, 8H, J=4.6 Hz, β-H), and 10.16 (s, 4H, *meso*-H); MALDI-TOF-MS calcd for $C_{354}H_{370}N_{24}O_{12}Zn_6$: 5532.48, found: 5538.10; UV–vis ($CHCl_3$): λ_{max}=418, 458, and 552 nm.

4.1.3. 1,3,5-Trioxamethylbenzene-bridged *meso–meso* linked porphyrin triple dimer (hexamer) 5. Compound **4** (20 mg, 0.0036 mmol) was dissolved in $CHCl_3$ (2000 mL) and the reaction vessel was covered with foil. A solution of 0.1 M $AgPF_6$ in CH_3CN (0.0072 mmol) was added and the mixture was stirred for 36 h at room temperature under Ar atmosphere. The same work-up procedure for **4** gave **5** (7.6 mg, 38%). ^1H NMR (CD_2Cl_2, 600 MHz): δ=−0.47 to −0.34 (m, 54H, ^{t}Bu), 0.42–0.54 (m, 54H, ^{t}Bu), 1.37–1.44 (m, 108H, ^{t}Bu), 3.96–3.99 (m, 12H, CH_2), 4.37 (m, 12H, CH_2), 4.62–4.73 (m, 12H, CH_2), 5.65 (s, 6H, Ar-H), 7.31 (s, 6H, Ar-H), 7.37–7.39 (m, 12H, Ar-H),

7.57 (s, 6H, spacer-H), 7.68–7.74 (m, 18H, Ar-H), 7.75 (s, 6H, Ar-H), 7.90 (d, 6H, J=4.4 Hz, β-H), 8.05 (s, 6H, Ar-H), 8.10 (s, 6H, Ar-H), 8.18–8.23 (m, 12H, β-H), 8.54 (d, 6H, J=4.6 Hz, β-H), 8.71 (d, 6H, J=4.5 Hz, β-H), 8.83 (d, 6H, J=4.5 Hz, β-H), 9.00 (d, 6H, J=4.6 Hz, β-H), and 9.03 (d, 6H, J=4.6 Hz, β-H); MALDI-TOF-MS calcd for $C_{354}H_{366}N_{24}O_{12}Zn_6$: 5528.45, found: 5533.46; UV–vis ($CHCl_3$): λ_{max}=423, 453, and 555 nm.

4.1.4. 1,3,5-Trioxamethylbenzene-bridged *meso–meso*, β–β, β–β linked porphyrin triple dimer (hexamer) 6. Compound **5** (4.0 mg, 0.72 μmol) was oxidized with DDQ (2.4 mg, 10.8 μmol) and $Sc(OTf)_3$ (5.2 mg, 10.8 μmol) in toluene (6 mL) at 60 °C for 12 h under N_2 atmosphere. THF was added and the mixture was stirred for additional 1 h. The mixture was directly passed through an alumina column and the solvent was evaporated. The residue was recrystallized from CH_2Cl_2/CH_3CN. Compound **6** (2.4 mg, 0.43 μmol, 48%) was obtained. ^{1}H NMR (CD_2Cl_2 with n-$BuNH_2$, 600 MHz): δ=1.37–1.44 (m, 216H, ^{t}Bu), 3.53–3.65 (m, 12H, CH_2), 3.90–4.08 (m, 12H, CH_2), 4.32–4.49 (m, 12H, CH_2), 6.73–6.80 (m, 6H, Ar-H), 6.85–6.87 (m, 6H, Ar-H), 6.95–7.00 (m, 6H, spacer-H), 7.02–7.11 (m, 12H, Ar-H), 7.16–7.22 (m, 12H, Ar-H), and 7.25–7.80 (m, 60H, β-H, Ar-H), MALDI-TOF-MS calcd for $C_{354}H_{354}N_{12}O_{12}Zn_6$: 5516.36, found: 5520.35; UV–vis ($CHCl_3$): λ_{max}=418, 463, 558, 957, and 1185 nm.

4.1.5. Zn(II) porphyrin pentamer 11. A mixture of **1** (257 mg, 0.330 mmol), **10** (47.9 mg, 0.0412 mmol), and K_2CO_3 (336 mg, 2.44 mmol) in dry acetone (50 mL) was refluxed for 4 days. H_2O was added and the mixture was extracted with CH_2Cl_2. The combined organic layer was dried with Na_2SO_4 and evaporated. The residue was purified with silica gel column chromatography (Wako 300 mesh, CH_2Cl_2/hexane). Separation over recycling preparative GPC–HPLC gave the free-base pentamer. The free-base pentamer was dissolved with $CHCl_3$ and $Zn(OAc)_2$ and refluxed for 5 h. The solution was washed with water and the organic layer was dried with Na_2SO_4 and evaporated. After passed through a short silica gel column and evaporated, the residue was recrystallized from CH_2Cl_2/MeOH to give porphyrin pentamer **11** (87.3 mg, 0.0221 mmol, 54%). ^{1}H NMR ($CDCl_3$, 600 MHz): δ=1.42–1.45 (m, 144H, ^{t}Bu), 2.08–2.32 (m, 8H, CH_2), 4.01–4.32 (m, 16H, CH_2), 6.97–7.10 (m, 4H, Ar-H), 7.30–7.47 (m, 8H, Ar-H), 7.57–7.63 (m, 8H, Ar-H), 7.67–7.73 (m, 20H, Ar-H), 7.97–8.03 (m, 16H, Ar-H), 8.77–8.85 (m, 8H, β-H), 8.88–8.97 (m, 16H, β-H), 9.03–9.08 (m, 8H, β-H), 9.26–9.36 (m, 8H, β-H), and 10.10–10.17 (m, 4H, *meso*-H), MALDI-TOF-MS calcd for $C_{272}H_{268}N_{20}O_8Zn_5$: 4261.76, found: 4265.80; UV–vis ($CHCl_3$): λ_{max}=418, and 547 nm.

4.1.6. Zn(II) porphyrin pentamer 12. Compound **11** (20 mg, 0.00468 mmol) was dissolved in $CHCl_3$ (800 mL), and the reaction vessel was covered with foil. To the solution was added a solution of 0.1 M $AgPF_6$ in CH_3CN (0.065 mmol) all at once and progress of reaction was monitored by analytical GPC–HPLC. After stirring for 14.5 h at room temperature, the mixture was diluted with water and the porphyrin products were extracted with $CHCl_3$. The organic extract was washed with water and dried over Na_2SO_4. After evaporation the residue was dissolved with $CHCl_3$ and metallated with $Zn(OAc)_2$. The desired compound was separated over a recycling preparative GPC–HPLC to give **12** (7.2 mg, 36%). ^{1}H NMR ($CDCl_3$ at 60 °C, 600 MHz): δ=1.23–1.30 (m, 72H, ^{t}Bu), 1.40–1.50 (m, 72H, ^{t}Bu-H), 2.20–2.48 (m, 8H, CH_2), 3.89–4.00 (m, 8H, CH_2), 4.07–4.19 (m, 8H, CH_2), 6.44–6.56 (m, 4H, β-H), 6.75–6.83 (m, 4H, Ar-H), 6.88–6.91 (m, 4H, Ar-H), 6.92–7.00 (m, 8H, Ar-H), 7.06–7.28 (m, 84, Ar-H), 7.30–7.36 (m, 8H, Ar-H), 7.53–7.63 (m, 4H, Ar-H), 7.71–7.76 (m, 4H, Ar-H), 7.77–7.82 (m, 8H, Ar-H), 7.83–7.93 (m, 4H, β-H), 8.01–8.06 (m, 4H, Ar-H), 8.15–8.23 (m, 4H, Ar-H), 8.30–8.34 (m, 4H, Ar-H), 8.36–8.47 (m, 8H, β-H), 8.69–8.83 (m, 8H, β-H), 8.87–8.91 (m, 4H, β-H), 8.97–9.04 (m, 4H, β-H), and 9.07–9.20 (m, 8H, β-H); MALDI-TOF-MS calcd for $C_{272}H_{264}N_{20}O_8Zn_5$: 4257.73, found: 4262.87; UV–vis ($CHCl_3$): λ_{max}=423, 453, and 555 nm.

4.1.7. Zn(II) porphyrin pentamer 13. Compound **12** (24.8 mg, 5.8 μmol) was oxidized with DDQ (13.2 mg, 58 μmol) and $Sc(OTf)_3$ (28.5 mg, 58 μmol) in toluene (6 mL) at 60 °C and reaction progress was monitored by analytical GPC–HPLC. The solution was stirred for 36 h under N_2. Then THF was added to the reaction mixture and the solution was stirred for another 2 h. After evaporation of solvent the residue was dissolved with THF and the solution was directly passed through an alumina column and evaporated. After short silica gel column, the residue was separated over a recycling preparative GPC–HPLC to give **13** (2.5 mg, 10%). ^{1}H NMR ($CDCl_3$, 600 MHz): δ=1.20–1.28 (m, 72H, ^{t}Bu), 1.30–1.37 (m, 72H, ^{t}Bu), 1.95–2.01 (m, 8H, CH_2), 4.09–4.20 (m, 8H, CH_2), 4.24–4.33 (m, 8H, CH_2), 6.88 (s, 8H, β-H), 6.98–7.00 (m, 4H, Ar-H), 7.04–7.07 (m, 4H, Ar-H), 7.07–7.09 (m, 4H, Ar-H), 7.10–7.18 (m, 12H, Ar-H), 7.34–7.41 (m, 16H, Ar-H), 7.42–7.65 (m, 32H, Ar-H, β-H), and 8.37 (s, 8H, β-H); MALDI-TOF-MS calcd for $C_{272}H_{256}N_{20}O_8Zn_5$: 4249.67, found: 4254.32; UV–vis ($CHCl_3$): λ_{max}=420, 562, 585, and 1071 nm.

Acknowledgements

This work was supported by Grant-in-Aids for Scientific Research on Priority Area (No. 18033028, Coordination Space) from the Ministry of Education, Culture, Sports, Science and Technology of Japan.

References and notes

1. (a) Wasielewski, M. R. *Chem. Rev.* **1992**, *92*, 435–461; (b) Gust, D.; Moore, T. A.; Moore, A. L. *Acc. Chem. Res.* **1993**, *26*, 198–205; (c) Gust, D.; Moore, T. A.; Moore, A. L. *Acc. Chem. Res.* **2001**, *34*, 40–48; (d) Holten, D.; Bocian, D.; Lindsey, J. S. *Acc. Chem. Res.* **2002**, *35*, 57–69; (e) Burrell, A. K.; Officer, D. L.; Plieger, P. G.; Reid, D. C. W. *Chem. Rev.* **2001**, *101*, 2751–2796; (f) Aratani, N.; Osuka, A. *Bull. Chem. Soc. Jpn.* **2001**, *74*, 1361–1379; (g) Yeow, E. K. L.; Ghiggino, K. P.; Reek, J. N. H.; Crossley, M. J.; Bosman, A. W.; Schenning, A. P. H. J.; Meijer, E. W. *J. Phys. Chem. B* **2000**, *104*, 2596–2606; (h) Choi, M.-S.; Aida, T.; Yamazaki, Y.; Yamazaki, I. *Chem.—Eur. J.* **2002**, *8*, 2668–2678.
2. (a) Osuka, A.; Shimidzu, H. *Angew. Chem., Int. Ed.* **1997**, *36*, 135–137; (b) Aratani, N.; Osuka, A.; Kim, Y. H.; Jeong,

D. H.; Kim, D. *Angew. Chem., Int. Ed.* **2000**, *39*, 1458–1462; (c) Kim, Y. H.; Jeong, D. H.; Kim, D.; Jeoung, S. C.; Cho, H. S.; Kim, S. K.; Aratani, N.; Osuka, A. *J. Am. Chem. Soc.* **2001**, *123*, 76–86.
3. Yoshida, N.; Osuka, A. *Org. Lett.* **2000**, *2*, 2963–2966.
4. Peng, X.; Aratani, N.; Takagi, A.; Matsumoto, T.; Kawai, T.; Hwang, I.-W.; Ahn, T. K.; Kim, D.; Osuka, A. *J. Am. Chem. Soc.* **2004**, *126*, 4468–4469.
5. Hori, T.; Aratani, N.; Takagi, A.; Matsumoto, T.; Kawai, T.; Yoon, M.-C.; Yoon, Z. S.; Cho, S.; Kim, D.; Osuka, A. *Chem.—Eur. J.* **2006**, *12*, 1319–1327.
6. (a) Tsuda, A.; Osuka, A. *Science* **2001**, *293*, 79–82; (b) Tsuda, A.; Osuka, A. *Adv. Mater.* **2002**, *14*, 75–79; (c) Tsuda, A.; Furuta, H.; Osuka, A. *J. Am. Chem. Soc.* **2001**, *123*, 10304–10321.
7. (a) Kim, D. Y.; Ahn, T. K.; Kwon, J. H.; Kim, D.; Ikeue, T.; Aratani, N.; Osuka, A.; Shigeiwa, M.; Maeda, S. *J. Phys. Chem. A* **2005**, *109*, 2996–2999; (b) Ahn, T. K.; Kim, K. S.; Kim, D. Y.; Noh, S. B.; Aratani, N.; Ikeda, C.; Osuka, A.; Kim, D. *J. Am. Chem. Soc.* **2006**, *128*, 1700–1704.
8. Sato, H.; Tashiro, K.; Shinmori, H.; Osuka, A.; Murata, Y.; Komatsu, K.; Aida, T. *J. Am. Chem. Soc.* **2005**, *127*, 13086–13087.
9. Bonifazi, D.; Spillmann, H.; Kiebele, A.; de Wild, M.; Seiler, P.; Cheng, F.; Güntherodt, H.-J.; Jung, T.; Diederich, F. *Angew. Chem., Int. Ed.* **2004**, *43*, 4759–4763.
10. (a) Nakano, A.; Osuka, A.; Yamazaki, I.; Yamazaki, T.; Nishimura, Y. *Angew. Chem., Int. Ed.* **1998**, *37*, 3023–3027; (b) Nakano, A.; Yamazaki, T.; Nishimura, Y.; Yamazaki, I.; Osuka, A. *Chem.—Eur. J.* **2000**, *6*, 3254–3271.
11. An, H.; Bradshaw, J. S.; Krakowiak, K. E.; Tarbet, B. J.; Dalley, N. K.; Kou, X.; Zhu, C.; Izatt, R. M. *J. Org. Chem.* **1993**, *58*, 7694–7699.
12. Seybold, P. G.; Gouterman, M. *J. Mol. Spectrosc.* **1969**, *31*, 1–13.
13. Kasha, M.; Rawls, H. R.; El-Bayoumi, M. A. *Pure Appl. Chem.* **1965**, *11*, 371–392.
14. (a) Yoshida, N.; Ishizuka, T.; Osuka, A.; Jeong, D. H.; Cho, H. S.; Kim, D.; Matsuzaki, Y.; Nogami, A.; Tanaka, K. *Chem.—Eur. J.* **2003**, *9*, 58–75; (b) Shinmori, H.; Ahn, T. K.; Cho, H. S.; Kim, D.; Yoshida, N.; Osuka, A. *Angew. Chem., Int. Ed.* **2003**, *42*, 2754–2758.
15. (a) Ahn, T. K.; Yoon, Z. S.; Hwang, I.-W.; Lim, J. K.; Rhee, H.; Joo, T.; Sim, E.; Kim, S. K.; Aratani, N.; Osuka, A.; Kim, D. *J. Phys. Chem. B* **2005**, *109*, 11223–11230; (b) Park, M.; Cho, S.; Yoon, Z. S.; Aratani, N.; Osuka, A.; Kim, D. *J. Am. Chem. Soc.* **2005**, *127*, 15201–15206; (c) Park, M.; Yoon, M.-C.; Yoon, Z. C.; Hori, T.; Peng, X.; Aratani, N.; Hotta, J.; Ujiki, H.; Sliwa, M.; Hofkens, J.; Osuka, A.; Kim, D. *J. Am. Chem. Soc.* **2007**, *129*, 3539–3544.
16. (a) Abdalmuhdi, I.; Chang, C. K. *J. Org. Chem.* **1985**, *50*, 411–413; (b) Nagata, T.; Osuka, A.; Maruyama, K. *J. Am. Chem. Soc.* **1990**, *112*, 3054–3059.
17. Albota, M.; Beljonne, D.; Brédas, J.-L.; Ehrlich, J. E.; Fu, J.-Y.; Heikal, A. A.; Hess, S. E.; Kogej, T.; Levin, M. D.; Marder, S. R.; McCord-Maughon, D.; Perry, J. W.; Röckel, H.; Rumi, M.; Subramaniam, G.; Webb, W. W.; Wu, X.-L.; Xu, C. *Science* **1998**, *281*, 1653–1656.
18. (a) Bartholomew, G. P.; Bazan, G. C. *Acc. Chem. Res.* **2001**, *34*, 30–39; (b) Woo, H. Y.; Hong, J. W.; Liu, B.; Mikhailovsky, A.; Korystov, D.; Bazan, G. C. *J. Am. Chem. Soc.* **2005**, *127*, 820–821.